CERN-INTC-2023-071 / INTC-P-679
26/09/2023

EUROPEAN ORGANIZATION FOR NUCLEAR RESEARCH

Proposal to the ISOLDE and Neutron Time-of-Flight Committee

Search for shape coexistence in ^{80}Zn via (t,p) reactions

S. Bottoni[1], F. Galtarossa[2], K. Wimmer[3], L. P. Gaffney[4], D. K. Sharp[5], P. Aguilera[2], F. Angelini[2,6], M. Balogh[6], J. Benito[2], G. Benzoni[1], A. Bracco[1], D. Brugnara[6], P. Butler[4], F. Camera[1], S. Carollo[2], G. Ciconali[1], G. Corbari[1], F. C. L. Crespi[1], G. De Angelis[6], R. Escudeiro[2], S. Freeman[5], A. Giaz[1], A. Goasduff[6], B. Góngora-Servín[6], A. Gottardo[6], B. Kay[7], M. Labiche[8], J. A. Lay-Valera[9], I. Lazarus[8], S. Leoni[1], S. Lenzi[2], M. Luciani[1], N. Marchini[10], R. Menegazzo[2], D. Mengoni[2], B. Million[1], A. Nannini[10], F. Nowacki[11], R. Page[4], J. Pellumaj[6], R. M. Pérez-Vidal[6], S. Pigliapoco[2], E. Pilotto[2], M. Polettini[2], R. Raabe[12], F. Recchia[2], K. Rezynkina[2], M. Rocchini[10], O. Tengblad[13], J. J. Valiente-Dobón[6], O. Wieland[1], L. Zago[2,6]

[1] *Università degli Studi di Milano and INFN Milano, Milano, Italy*
[2] *Università degli Studi di Padova and INFN Padova, Padova, Italy*
[3] *GSI, Darmstadt, Germany*
[4] *University of Liverpool, Liverpool, UK*
[5] *University of Manchester, Manchester, UK*
[6] *INFN Laboratori Nazionali di Legnaro, Legnaro, Italy*
[7] *Argonne National Laboratory, Lemont, USA*
[8] *STFC, Daresbury Laboratory, Daresbury, UK*
[9] *University of Sevilla, Sevilla, Spain*
[10] *INFN Firenze, Firenze, Italy*
[11] *Université de Strasbourg, IPHC, Strasbourg, France*
[12] *IKS, KU Leuven, Leuven, Belgium*
[13] *Instituto Estructura de la Materia, CSIC, Madrid, Spain*

Spokesperson: S. Bottoni (simone.bottoni@mi.infn.it)
Spokesperson: F. Galtarossa (franco.galtarossa@pd.infn.it)
Contact person: P. MacGregor (patrick.macgregor@cern.ch)

Abstract: We propose to probe shape coexistence in ^{80}Zn, located along the $N = 50$ shell closure and only two protons away from the doubly-magic ^{78}Ni nucleus, by searching, in particular, for the 0_2^+ excited state. The latter is predicted by shell-model calculations at 2.15 MeV, with sizable deformation originating from two-particle-two-hole excitations across the $N = 50$ shell gap. We intend to employ the ^{78}Zn(t,p), two-neutron-transfer reaction which will selectively favour the population of such neutron configurations. The experiment will be performed with the Isolde Solenoid Spectrometer, using a ^{78}Zn beam at 6 MeVA impinging on a ^{3}H radioactive target. The ^{80}Zn excitation energy will be reconstructed through the detected energy and angle of emitted protons, whereas 0^+ states will be identified by measuring proton angular distributions with distinctive features of a $\Delta L = 0$ transfer.

Requested shifts: 24 shifts (3 setup + 21 experiment)

1 Physics case

Nowadays, shape coexistence is considered to be a well-established phenomenon, expected to appear in the majority of atomic nuclei located in the proximity of closed shells [1, 2]. The experimental study of shape coexistence far from stability, where only few spectroscopic data are available, is of paramount importance to benchmark modern nuclear models and interactions aimed at providing a theoretical microscopic description of nuclear shapes [3, 4]. This is ultimately related to the nature of nuclear forces, which drive shell evolution and proton-neutron correlations, leading to the stabilization of both deformed configurations and spherical structures at similar excitation energy.
In the medium-mass region of the nuclide chart, remarkable results were achieved along the Ni ($Z = 28$) isotopic chain, in the vicinity of the $N = 40$ subshell closure. A triple shape coexistence was established in ^{68}Ni [5] and several excited 0^+ states, with different degrees of deformation, were discovered to coexist at low energy in ^{66}Ni and ^{64}Ni [6, 7]. These are well described by Monte-Carlo Shell-Model calculations, which point to the role of the monopole component of the tensor force to steady deformed structures [8]. On the other hand, experimental information on shape coexistence around the next − and much more exotic − shell closure at $N = 50$ is still rather scarce. In-beam γ-ray spectroscopy data in ^{78}Ni revealed its doubly-magic nature, probing, at the same time, the existence of a side band along with yrast states [9]. The latter were interpreted by shell model calculations to be of spherical shape, built on one-particle-one-hole ($1p-1h$) neutron excitations across the $N = 50$ shell gap, whereas the measured (2^+_2) state at 2.91 MeV was suggested to be prolate deformed. Its wave function is predicted to be dominated by $2p-2h$ neutron excitations and, although not observed, a 0^+_2 deformed bandhead state is proposed by shell-model calculations, using the PFSDG-U interaction, at 2.65 MeV [4, 10, 11] and by Monte-Carlo Shell-Model calculations at 2.61 MeV [9].
In the region around ^{78}Ni, only a few cases of possible shape coexistence were reported up to now. The deformed nature of the low-lying $1/2^+$ isomeric state in ^{79}Zn at $N = 49$ was established in a g-factor measurement with LASER spectroscopy at ISOLDE [12]. Its large isomer shift points to a quadrupole deformation with $\beta_2 = 0.22$, twice as large as the ground state one ($\beta_2 \approx 0.14$). This state is interpreted as a $N = 50$ intruder level with a $\nu(g^{-2}_{9/2}s^1_{1/2})$ configuration. Moreover, in ^{80}Ge at $N = 48$, a 0^+_2 deformed state was originally proposed in a β-decay measurement at 639 keV [13], yet a more recent β-γ experiment disproved the existence of such a state [14]. The non-observation of a low-lying 0^+ state was supported by shell-model calculations, predicting the 0^+_2 state at 2 MeV of excitation energy. This makes ^{79}Zn the only firm example of shape coexistence in the close proximity of ^{78}Ni.
In this experiment, we would like to search for the 0^+_2 state in ^{80}Zn (Z=30), and possibly other 0^+ excited states, to potentially extend the shape coexistence paradigm to this N=50 even-even system, closer to the doubly-magic ^{78}Ni nucleus. Probing shape coexistence in ^{80}Zn will shed light on the robustness of the N=50 shell closure and on the interplay between the possible quench of the single-particle gap and the effect of quadrupole correlations to stabilize deformed structures in this exotic mass region.

The evolution of nuclear shapes and collectivity in even-even Zn isotopes has attracted much attention in the last decade [15, 16, 17, 18, 19]. In ^{80}Zn, shape coexistence was predicted by shell-model calculations performed with the PFSDG-U interaction [10, 11]. A valence space made of the full pf shell for protons and the full sdg shell for neutrons was employed, using a ^{60}Ca inert core. Two low-lying 0^+ states were found, namely the spherical ground state and a deformed 0^+_2 state, with $\beta_2 \approx 0.2$, calculated at 2.16 MeV of excitation energy. The predicted proton and neutron occupancies for these two states are presented in Tab. 1, while the DNO-SM expansions in the (β,γ) plane are shown in the left panel of Fig. 1 [20]. From its wave-function composition, one can note that the structure of the 0^+_2 state is dominated by $2p-2h$ neutron excitations across $N = 50$, mainly from the $g_{9/2}$ orbital to the $d_{5/2}$ and $s_{1/2}$ orbitals, with an average number of 2.7 neutrons above the shell gap. On the other hand, both the 0^+_1 and 0^+_2 states have a similar number of protons in the $f_{5/2}p_{3/2}p_{1/2}$ shells, with a very little amount of particles promoted across the $Z = 28$ shell gap for the 0^+_2 state.

J^π	E_{exp}	E_{theo}	$\nu g_{9/2}$	$\nu d_{5/2}$	$\nu s_{1/2}$	$\nu g_{7/2}$	$\nu d_{3/2}$	$\pi f_{7/2}$	$\pi f_{5/2}$	$\pi p_{3/2}$	$\pi p_{1/2}$
0^+_1	0.0	0.0	9.50	0.23	0.03	0.19	0.04	7.52	1.90	0.44	0.14
0^+_2	-	2.16	7.26	1.20	0.71	0.52	0.31	6.92	1.33	1.28	0.47

Table 1: Occupation of orbitals in the full proton pf and neutron sdg valence space for low-lying 0^+ states in ^{80}Zn. E_{exp} and E_{theo} (in MeV) are the experimental and predicted excitation energies, respectively [10].

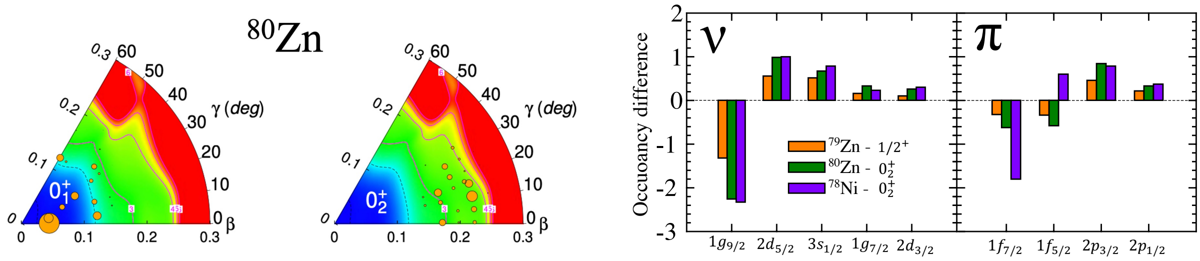

Figure 1: (Left) Discrete Non-Orthogonal shell-model (DNO-SM) expansions in the (β,γ) plane for the predicted 0^+_1 and 0^+_2 states in ^{80}Zn [10]. (Right) Proton and neutron occupancy differences for excited states in ^{79}Zn, ^{80}Zn and ^{78}Ni with respect to their ground states [10].

It is very interesting to note the striking similarities of the calculated 0^+_2 state in ^{80}Zn with the predicted structure of the $1/2^+$ state in ^{79}Zn and the one of the 0^+_2 state in ^{78}Ni, pointing to a similar deformation mechanism in these nuclei. The proton and neutron occupancy differences with respect to their ground states are shown in the right side of Fig. 1. The same dominant $(d_{5/2})^2$ and $(s_{1/2})^2$ neutron configurations are found, while the energy of the 0^+_2 state in ^{80}Zn is predicted to lower down compared with the 0^+_2 state in ^{78}Ni. This is due due to protons already occupying the $f_{5/2}$ orbital in ^{80}Zn, while $p-h$ excitations from the $\pi f_{7/2}$ are required in ^{78}Ni. Therefore, probing the 0^+_2 state in ^{80}Zn will also allow us to gain insights into the structure of the yet unobserved 0^+_2 state in the doubly-magic ^{78}Ni nucleus [9].

2 Proposed experiment

Given the expected $\nu(2p-2h)$ nature of the 0^+_2 state in ^{80}Zn, involving excitations from the $g_{9/2}$ orbital across the $N=50$ shell gap, we propose to use the ^{78}Zn(t,p) two-neutron transfer reaction to enhance the population of such a state. We note that (t,p) reactions in inverse kinematics were already employed successfully at ISOLDE to study the 0^+_2 state in ^{32}Mg [21], ^{46}Ar [22], and ^{66}Ni [23], even with low-energy and low-intensity radioactive beams.
The experiment will be performed at HIE-ISOLDE with the Isolde Solenoid Spectrometer (ISS) using a ^{78}Zn beam at 6 MeVA. Such a beam was already used in the IS491 experiment, with a reported intensity of $7.8(7)\cdot 10^5$ pps after post-acceleration and a purity of 75 % [24]. The beam will impinge on a tritium-loaded titanium foil, with a Ti thickness of 0.5 mg/cm^2, as the one used in Refs. [21, 22, 23]. The target is being produced by the SODERN company which already achieved a ^{3}H/Ti ratio of 0.4, with the aim of doubling it [25]. For the current proposal, we considered an average loading ratio of 0.6, corresponding to an effective ^{3}H thickness of $\sim 20\,\mu$g/cm^2.
Protons from the ^{78}Zn(t,p) reaction will be detected and identified at backward angles using the silicon array of the ISS setup. By setting the solenoid magnetic field to 2.5 T and placing the array between -200 mm and -700 mm from the target, we will be able to fully cover an angular range from about 8° to 50° in the center-of-mass reference frame (CM) for excitation energies in ^{80}Zn around 2 MeV, where the 0^+_2 state is expected. In general, we will be able to cover from 8° to 40° in the CM frame of reference for excitation energies up to 4 MeV. The calculated proton kinematic lines and the proton orbits in ISS are shown in Fig. 2. Light particles will be distinctively identified using their cyclotron frequency in the solenoid while heavy recoils will be detected by the newly-developed fast-counting ionization chamber mounted downstream. Moreover, the (t,t) elastic scattering will be also measured by a monitor detector and used as a normalization to determine absolute cross sections.
Differential cross sections for the ^{78}Zn(t,p) reaction were calculated with the FRESCO code using a DWBA approach [26]. In particular, for the 0^+_2 state, the direct transfer

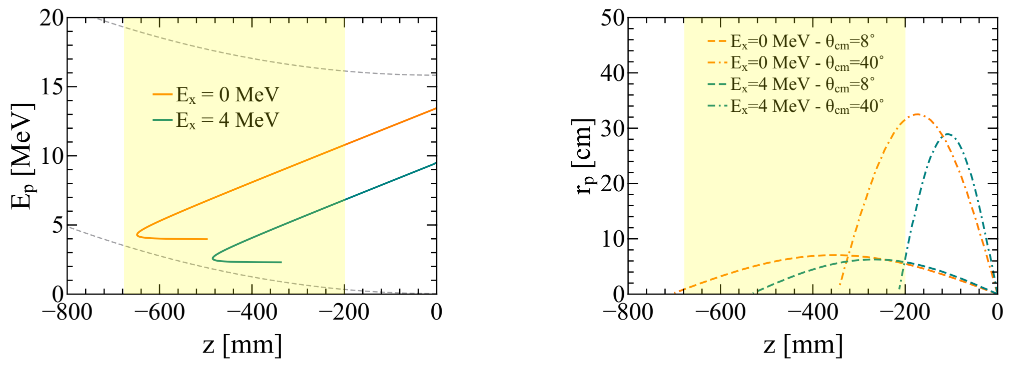

Figure 2: (Left) Proton kinematic lines for two states at 0 MeV and 4 MeV of excitation energy. (Right) Proton orbits for two states at 0 MeV and 5 MeV and center-of-mass angles from 8° to 40°. The coverage of the ISS Si array is displayed in yellow.

of a $(d_{5/2})^2$ and $(s_{1/2})^2$ neutron pair was considered, according to the shell-model wave function shown in Tab. 1. The resulting total integrated cross section for the population of the 0_2^+ in ^{80}Zn is ~ 0.3 mb. Preliminary second-order DWBA calculations were also performed to evaluate the relative contribution of the sequential and direct pair transfer and the possible interference of different two-nucleon amplitudes (TNA). Their impact on the absolute cross section turned out to be of the order of 30-40 %.
The 0_2^+ state will be identified by studying the angular distribution of the emitted protons, which will show the characteristic features of a $\Delta L = 0$ transfer. Its shape is well distinguishable from that of $\Delta L = 2$ transfers, which are also expected to be observed with the selected reaction. The response of the ISS setup in terms of efficiency and resolution was evaluated through GEANT4 simulations performed within the NPTool framework [27], for the population of the 0_1^+, 2_1^+ and 0_2^+ states in ^{80}Zn. The total efficiency of the array turned out to be about 30 % for $\Delta L = 0$ and 40 % for $\Delta L = 2$ transfer. The excitation energy resolution is $\sim$ 300 keV (FWHM), mainly determined by the target thickness.

3 Counting rate estimates and beam time request

For the counting rate estimates we considered:

- Beam intensity: $5 \cdot 10^5$ pps;
- ^{3}H target thickness: 20 μg/cm^2 ($4.8 \cdot 10^{18}$ atoms/cm^2);
- A total integrated cross section for the 0_2^+ state in ^{80}Zn of 0.3 mb;
- A total ISS efficiency of $\sim$ 30 % for $\Delta L = 0$ transfer, with the Si array covering from -700 to -200 mm.

To detect approximately 100 protons coming from the transfer to the 0_2^+ state, 7 days of beam time are required. The expected excitation energy spectrum is shown in the left panel of Fig. 3, while the right panel shows the angular distributions for $\Delta L = 0$ and $\Delta L = 2$ transfers. The experimental points and error bars are derived from the analysis of the simulated data with the statistics expected in the requested beam time. This will allow us to clearly distinguish between $\Delta L = 0$ and $\Delta L = 2$ transfer and to extract the relative contributions of the $(d_{5/2})^2$ and $(s_{1/2})^2$ components to compare with shell-model predictions, as done in Refs.[21, 22, 23]. We also intend to explore the higher excitation energy region of ^{80}Zn, up to 4 MeV, to possibly identify other low-spin states which are currently unknown.

Summary of requested shifts: we request a total of **24 shifts**, divided in: 3 shifts for detector setup and 21 shifts to perform the experiment.

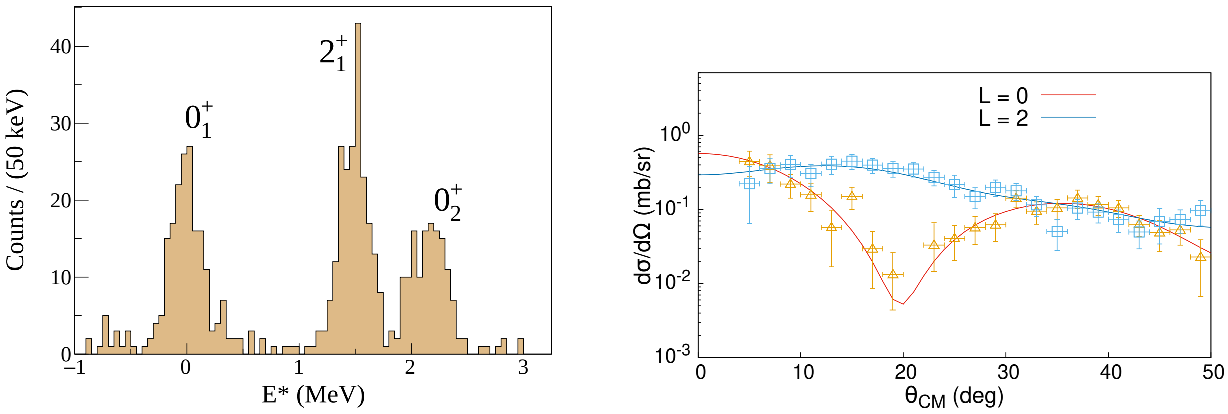

Figure 3: (Left) Simulated excitation energy spectrum for ^{80}Zn with the expected statistics in the requested beam time. (Right) Angular distributions for the $\Delta L = 0$ transfer to the 0_2^+ state (red) and $\Delta L = 2$ to the 2_1^+ state (blue).

References

[1] K. Heyde and J. L. Wood, Rev. Mod. Phys. **83**, 1467 (2011).

[2] P. E. Garrett *et al.*, Prog. Part. Nucl. Phys. **124**, 103931 (2022).

[3] T. Otsuka *et al.*, Rev. Mod. Phys. **92**, 015002 (2020).

[4] F. Nowacki *et al.*, Phys. Rev. Lett. **117**, 272501 (2016).

[5] B. P. Crider *et al.*, Phys. Lett. B **763**, 108 (2016).

[6] S. Leoni *et al.*, Phys. Rev. Lett. **118**, 162502 (2017).

[7] N. Marginean *et al.*, Phys. Rev. Lett. **125**, 102502 (2020).

[8] S. Suchyta *et al.*, Phys. Rev. C **89**, 021301(R) (2014).

[9] R. Taniuchi *et al.*, Nature **569**, 53 (2019).

[10] F. Nowacki, private communication.

[11] L. Nies *et al.*, accepted in Physcal Review.

[12] X. F. Yang *et al.*, Phys. Rev. Lett. **116**, 182502 (2016).

[13] A. Gottardo *et al.*, Phys. Rev. Lett. **116**, 182501 (2016).

[14] F. H. Garcia *et al.*, Phys. Rev. Lett. **125**, 172501 (2020).

[15] J. Van de Walle *et al.*, Phys. Rev. C **79**, 014309 (2009).

[16] C. Louchart *et al.*, Phys. Rev. C **87**, 054302 (2013)

[17] Y. Shiga *et al.*, Phys. Rev. C **93**, 024320 (2016).

[18] S. Hellgartner *et al.*, Phys. Lett. B **841** 137933 (2023).

[19] M Rocchini et al., Phys. Rev. Lett. **130**, 122502 (2023).

[20] D. D. Dao and F. Nowacki, Phys. Rev. C **105**, 054314 (2022).

[21] K. Wimmer *et al.*, Phys. Rev. Lett. **105**, 252501 (2010).

[22] K. Nowak *et al.*, Phys. Rev. C **93**, 044335 (2016).

[23] F. Flavigy et al., Phys. Rev. C **99**, 054332 (2019).

[24] R. Orlandi *et al.*, Phys. Lett. B **740**, 298 (2015).

[25] K. Wimmer, private communication.

[26] I. Thomson, *http://www. fresco.org.uk*

[27] A. Matta *et al.*, J. Phys. G: Nucl. Part. Phys. **43**, 045113 (2016).

DESCRIPTION OF THE PROPOSED EXPERIMENT

Please describe here below the main parts of your experimental set-up:

Part of the experiment	Design and manufacturing
ISOLDE Solenoidal Spectrometer	☒ To be used without any modification
If relevant, describe here the name of the flexible/transported equipment you will bring to CERN from your Institute [Part 1 of experiment/ equipment]	☐ Standard equipment supplied by a manufacturer ☐ CERN/collaboration responsible for the design and/or manufacturing
[Part 2 of experiment/ equipment]	☐ Standard equipment supplied by a manufacturer ☐ CERN/collaboration responsible for the design and/or manufacturing
[insert lines if needed]	

HAZARDS GENERATED BY THE EXPERIMENT

Additional hazard from flexible or transported equipment to the CERN site:

Domain	Hazards/Hazardous Activities		Description
Mechanical Safety	Pressure	☐	[pressure] [bar], [volume][l]
	Vacuum	☐	
	Machine tools	☐	
	Mechanical energy (moving parts)	☐	
	Hot/Cold surfaces	☐	
Cryogenic Safety	Cryogenic fluid	☐	[fluid] [m3]
Electrical Safety	Electrical equipment and installations	☐	[voltage] [V], [current] [A]
	High Voltage equipment	☐	[voltage] [V]
Chemical Safety	CMR (carcinogens, mutagens and toxic to reproduction)	☐	[fluid], [quantity]
	Toxic/Irritant	☐	[fluid], [quantity]
	Corrosive	☐	[fluid], [quantity]
	Oxidizing	☐	[fluid], [quantity]
	Flammable/Potentially explosive atmospheres	☐	[fluid], [quantity]
	Dangerous for the environment	☐	[fluid], [quantity]
Non-ionizing radiation Safety	Laser	☐	[laser], [class]
	UV light	☐	
	Magnetic field	☒	2.5 [T]
Workplace	Excessive noise	☐	
	Working outside normal working hours	☐	

	Working at height (climbing platforms, etc.)	☐	
	Outdoor activities	☐	
Fire Safety	Ignition sources	☐	
	Combustible Materials	☐	
	Hot Work (e.g. welding, grinding)	☐	
Other hazards			